

Open-Loop Experiments for Modeling the Human Eye Movement System

A. TERRY BAHILL, SENIOR MEMBER, IEEE, AND DEBORAH R. HARVEY

Abstract—Open-loop experiments were used to develop a linear model for a physiological system. The specific system studied was the eye movement system; however, the technique presented may be applied generally to other physical systems. Human smooth-pursuit eye movements were measured in response to sinusoidal, step, ramp, and step-ramp target motions in the normal closed-loop condition and in the open-loop condition. The human responses were compared to the outputs of four models, and the best match was provided by the $K/(\tau s + 1)$ model. Simulation results suggested that in the open-loop condition, the human often changed control strategy, for example by turning off the saccadic system and making no position-correcting saccades, in spite of large positional errors.

THE HUMAN smooth-pursuit eye movement system is a unique and enigmatic system. Although the system has a large time delay, humans can learn to track targets with no phase lag. They can do this if the target waveform is predictable, the velocity is continuous, and the acceleration is limited [1]. A simple example of such a waveform is a sinusoid. A complex example of such a waveform is a 90 mile per hour curveball thrown by a major league pitcher [2]. Traditionally the input to this system was considered to be target velocity, although position and acceleration may play a role [3], [4].

The technique of *opening a loop* on a system is an important tool in systems analysis. Therefore, it is not surprising that several recent papers have discussed opening the loop on the smooth pursuit system [5]–[10]. However, the results of these studies are confusing and contradictory.

This paper discusses the trials and tribulations of our open-loop experiments on the smooth pursuit system. The purpose of this research was to develop a model for this system. The purpose of this paper is to explain our technique. This paper could be used as a tutorial for constructing simple models of physical systems. Before discussing the experimental results, we think some detailed comments about opening a feedback loop are in order.

OPENING THE LOOP ON A SYSTEM

A linear system can be schematically represented as a closed-loop system, as shown in Fig. 1(a), or as an open-loop

system, as shown in Fig. 1(b). Consider the closed-loop system shown in Fig. 1(a). One common technique for studying such a system is to open the loop, as shown in Fig. 1(c), and then to study the response of the open-loop system. The open-loop transfer function is the total effect encountered by a signal as it travels around the loop, that is

$$G_{ol}(s) = G(s)H(s).$$

Note that this is not the input-output transfer function of the system with its loop opened (which would be $G(s)$), nor is this the transfer function of the equivalent intact open-loop system shown in Fig. 1(b). When we open the loop on a closed-loop system, bizarre behavior usually results. In response to a step disturbance, a closed-loop system with its loop opened will usually vary its output until some nonlinearity limits it. For instance, if $R(s)$ in Fig. 1(c) is a step and $G(s)$ is a pure integrator, the error will be constant and the output will increase linearly until the system becomes nonlinear.

Often the success of an engineering analysis depends on being able to open the loop on a system. If it is an electrical circuit, one might merely cut a wire. If it is a human physiological system, such an approach is not feasible, and other techniques must be developed [11], [12].

Saccadic System

There is an easy way to open the loop on the saccadic eye movement system. Look a few degrees to the side of a camera when someone triggers a flash. There will be an afterimage a few degrees off your fovea. Try to look at the afterimage. You will make a saccade of a few degrees, but the image (being fixed on the retina) will also move a few degrees. You will then make another saccade, and the image will move again. Thus, no matter how you move your eye, you cannot eliminate the error and put the image on your fovea. This is the same effect as if someone opened the loop on an electronic system by cutting a wire (Fig. 1(c)). Therefore, this is a way of opening the loop on the saccadic system. There is another simple way to study open-loop saccadic behavior. Gaze at the blue sky on a sunny day and try to track your floaters (sloughed collagen fibers in the vitreous humor). These hair-like images move when the eye moves; therefore, your initial saccades will not succeed in getting them on the fovea. However, with a little practice, one can learn to manipulate these images,

Manuscript received April 30, 1984; revised April 5, 1985 and December 4, 1985. This research was supported by the National Science Foundation under grant ECS-8121259.

A. T. Bahill is with the Department of Systems and Industrial Engineering, University of Arizona, Tucson, AZ 85721, USA.

D. R. Harvey is with the Mitre Corp., 1820 Dolly Madison Blvd, McLean, VA 22102, USA.

IEEE Log Number 8407461.

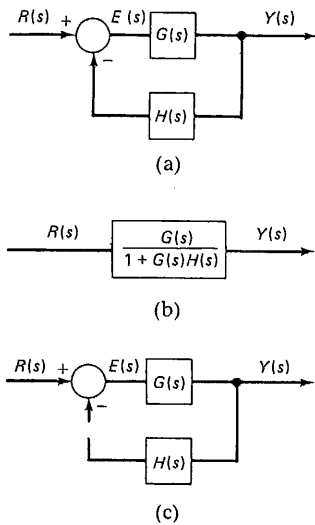


Fig. 1. (a) Closed-loop control system. (b) Equivalent open-loop representation. (c) Closed-loop representation with its loop opened. Many analysis techniques require the study of the open-looped system of (c). (From [12, p. 215]).

because they are not fixed on the retina and a human can rapidly learn to manipulate the system. This latter point often confounds attempts to open the loop on a physiological system. The experimenter closes a switch that supposedly opens the loop, but the human quickly changes control strategy, thus altering the system under study.

The most common experimental technique for opening the loop on the eye movement system, pioneered by Young and Stark in 1962 [13], employs electronic feedback as shown in Fig. 2. The position of the eye θ_E is continuously measured and is summated with the input target signal θ_T . For the eye movement system $H = 1$, because if the eye moves 10° , the image on the retina also moves 10° . If the eye movement monitor and associated amplifiers are carefully designed so that $H' = 1$, then any change in actual eye position is exactly cancelled by the change in measured eye position. Thus the error signal E is equal to the target signal. This is the same effect as if the feedback loop had been cut. The target position in space (TPS) is the sum of the input signal and the measured eye position; care must be taken to keep this position within the linear range of the eye movement monitor.

When this technique is used on the saccadic system, the target is given a small step displacement, say 2° to the right. After about 200 ms, the eyes saccade 2° to the right. During this movement, the target is moved 2° farther to the right, so that at the end of the saccade the target is still 2° to the right. After another 200-ms delay, the eyes saccade another 2° to the right, and the target is moved another 2° , maintaining the 2° retinal error. The saccadic eye movements are not effective in changing the retinal error; therefore the loop has been opened. In this open-loop condition the subject produces a staircase of 2° saccades about 200 ms apart, until the measuring system becomes nonlinear. This type of open-loop saccadic tracking is shown in Fig. 3.

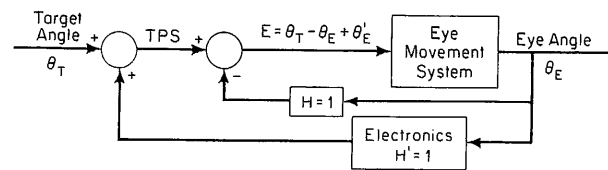


Fig. 2. Electronic technique for opening the loop on the human eye movement system.

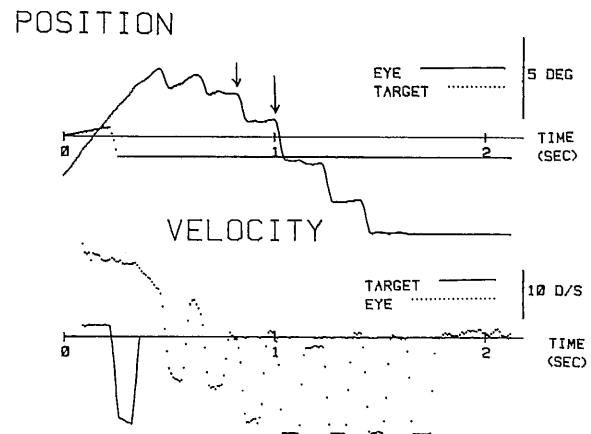


Fig. 3. Output of the saccadic system in the open-loop situation; the staircase of saccades is typical. The step target was presented immediately after an open-loop sine wave, which explains the position of the eye and target at the beginning of the data segment. The time between the arrows shows an example of measurement of the saccadic system latency.

Smooth-Pursuit System

Electronic feedback has also been used to open the loop on the smooth-pursuit system [5]. In these experiments the target was moved sinusoidally and the experimenters waited for the eye to respond. When the eye moved, they added the measured eye position signal to the sinusoidally moving target (as shown in Fig. 2). Thus the eye movements became ineffective in correcting the retinal error and the feedback loop was, in essence, opened. In contrast to open-loop saccadic experiments, open-loop smooth-pursuit experiments do not stabilize the image on the retina; but rather the target is moved across the retina in a controlled manner.

Leigh *et al.* [8] reported an unusual way of studying open-loop smooth-pursuit behavior in a patient with one paralyzed eye. They presented the target to the paralyzed eye while the movements of the mobile eye were monitored. This is a clever technique, but clearly it cannot be used with normal subjects.

MODEL FOR OPEN-LOOP DATA

Modeling is circular; the form of the model must be assumed before the experimental data can be analyzed and used to make the model. For example, a common way to model a system is to apply sinusoidal inputs of varying frequencies, record the output of the system, and construct Bode diagrams for the ratio of the output to the input. But this already assumes the form of the model; i.e., a linear system. To illustrate further, suppose you applied an input

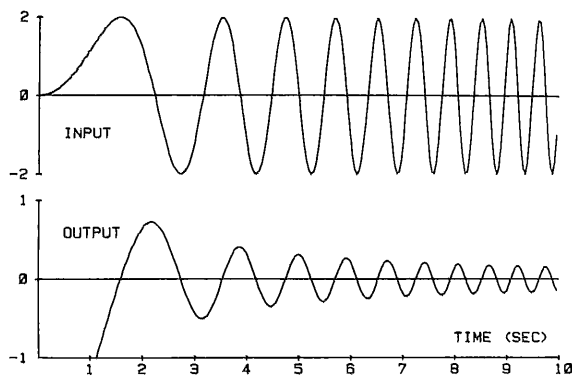


Fig. 4. Input and output of a hypothetical system that could be modeled as either a time-varying system, a nonlinear system, or a linear system.

of $r = 2 \sin \omega t$ sweeping the frequency between 0 and 1 Hz in 10 s, i.e., $f = t/10$. And you found the resulting output to be $y = (-1/\omega) \cos \omega t$, as shown in Fig. 4. Because we are looking for a transfer function, we would ignore the transients in the first second. If we also ignored phase information, three models for this system would pop into mind.

1) *Time Varying System*: $G = -5/(2\pi t)$, where the gain is a function of time.

2) *Nonlinear System*: $G = -2/\text{velocity}$, where the gain is a function of input velocity.

3) *Linear System*: $G = -1/2s$, where the gain is a function of frequency.

The choice between these three is usually made before the experimental data are analyzed.

Most engineering studies assume linear systems and plot gain as a function of frequency. However [5], [8] implicitly assumed a nonlinear model and plotted gain as a function of target velocity. Nonetheless, as shown above, if there are no *a priori* data to suggest otherwise, then the system can be analyzed more easily as a linear system. For example, the open-loop gains G_{ol} of [5], [8] can be fit by either the nonlinear function $G_{ol} = 4/\hat{\theta}_T$ as they did, or by the linear function $G_{ol} = 0.2/j\omega$, where ω is stimulus frequency and $\hat{\theta}_T$ is target velocity. The point is, if your model for the system is linear, then the open-loop gain data should be plotted as a function of frequency; if your model is nonlinear, then the open-loop gain data can be plotted as a function of target velocity, or any other appropriate variable.

Wyatt and Pola [6] assumed a linear model to analyze their data; they plotted their open-loop gains as a function of frequency. However, their open-loop gains were unusually high, often over ten. Most studies report open-loop gains ranging from four (at $2^\circ/\text{s}$) to two (at $10^\circ/\text{s}$), while Wyatt and Pola's ratio ranged from about 12 to five over the same interval. When Mack *et al.* [7] attempted to replicate Wyatt and Pola's experiment, they found open-loop gains in the four to two range. We think this discrepancy results from the subjects' varying degrees of prior experience in eye movement experiments. Because in Wyatt and Pola's subsequent study [9], the authors themselves had large open-loop gains, but their naive subjects had

gains in the normal range. And in our experiments, our most experienced subject (ATB) had open-loop gains more than twice as large as our other subjects.

Such intersubject variabilities led Cushman *et al.* [10] to conclude that

...caution is necessary when drawing inferences about human oculomotor system characteristics from [open-loop] experiments. This conclusion agrees with Tammings's conclusion that '...in an open-loop condition pursuit eye movements primarily reflect idiosyncrasies of the particular subject used in the experiment.'

Although open-loop experiments are difficult to perform, in this paper we will show that it is possible to get meaningful results; that is, individual behavior that is repetitive from day to day, with intersubject differences dependent only on the subject's experience.

MODELS FOR THE SMOOTH-PURSUIT SYSTEM

The purpose of running open-loop experiments is to derive data to help model the system. So before developing our model, let us review some previous models of the human smooth-pursuit system. The earliest model for the smooth pursuit branch is the sampled data model developed by Young and Stark [13]. As a result of more recent evidence [14], [15] the pursuit branch is no longer viewed as a sampled data system but rather as a continuous one.

There is one physically realizable model capable of overcoming the time delay in the smooth pursuit branch and producing zero-latency tracking; the target-selective adaptive control model (TSAC) [16]–[18] shown in Fig. 5. The exact details of this model are not important, so we will only present a short explanation for the various elements.

The input to the smooth-pursuit branch is velocity, *ergo*, the first differentiator. The limiter prevents any velocities greater than $70^\circ/\text{s}$ from going through this branch. Lisberger *et al.* [4] call this element an acceleration saturating nonlinearity. The next element, $K/(\tau s + 1)$, a first-order lag called a leaky integrator, was suggested by three experimental results. First, humans can track ramps with zero steady-state error [19]–[23]. Second, open-loop experiments have demonstrated that the frequency response of the smooth pursuit branch has a slope of approximately -20 dB per decade [6]. Third, eye acceleration is directly proportional to retinal error velocity [4]. The anatomical location for this leaky integrator is most likely the brain stem [24]. The closed-loop gain of the smooth-pursuit system is about unity. Therefore, the gain K must be greater than one; it has been estimated from open-loop experiments to be between two and four [7], [25], [26].

The e^{-sT} term represents the time delay in the system; a value of about 150 ms is currently accepted. The saturation element prevents the output of any velocities greater than $60^\circ/\text{s}$, the maximum velocity produced by the pursuit branch of most humans. The final integrator changes velocity signals into the position signals used by the extraocular plant.

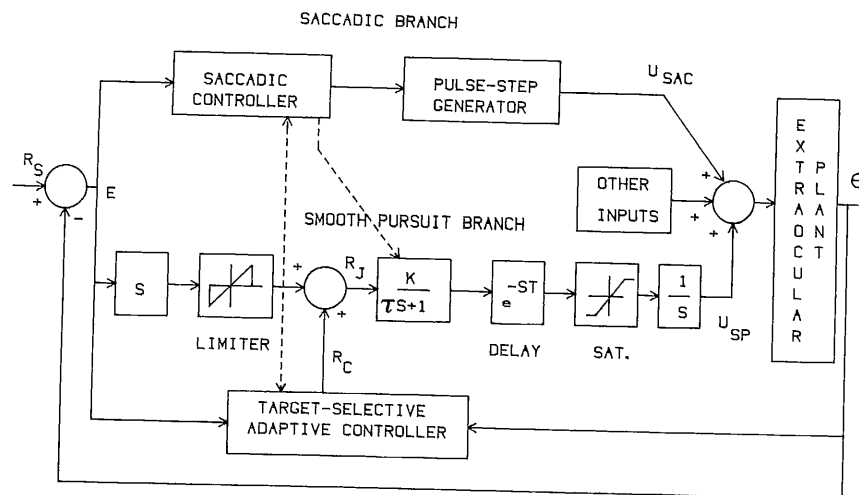


Fig. 5. Target-selective adaptive control model.

The smooth-pursuit models of Young *et al.* [27], [28] added a corollary discharge pathway to give eye position information in addition to retinal error information. The TSAC model also included a pathway providing eye position information. However, in this model the information was processed by the adaptive controller before it was sent to the smooth-pursuit branch. This additional processing element allowed open-loop experiments to be performed on the model. Several investigators have suggested that perceived target velocity is the stimulus for the smooth-pursuit system [29]. In this context R_J of Fig. 5 represents this perceived velocity. The adaptive controller of Fig. 5 must be able to predict future target velocity, and it must know and compensate for the dynamics of the rest of the system [18].

Our experiments were designed to eliminate the effects of most of these elements; we only studied the effects of $Ke^{-sT}/(\tau s + 1)$. The adaptive controller was eliminated by using unpredictable target waveforms or by only looking at the first few seconds of tracking. A unique target waveform (to be described later) eliminated the need for the saccadic system. And the limiter and saturation elements were eliminated by using low target velocities.

The original TSAC model used a gain of 4 and a pure integrator in the forward path of the pursuit branch. However, this combination yielded a closed-loop time constant of 250 ms, and our start-up transient data indicated that this time constant should be smaller. The purpose of this research was to find a better model for this element. We considered the following: a pure integrator, (K/s) ; a first order lag, $K/(\tau s + 1)$; a critically damped second-order system; and an overdamped second-order system. Our experiments helped determine the form of the model and the parameter values.

EXPERIMENTAL METHODS

We used the DDA dark pupil Oculometer to measure eye movements [30]. It used an $X - Y$ photodiode (Selcom Co., type 2L24) to detect the horizontal and vertical position of the centroid of the pupil. The pupil was il-

luminated by infrared light. The infrared light and the image of the eye were reflected off an infrared mirror, so that the only intrusion in the subject's field of view was the infrared mirror, which appeared as a lightly tinted piece of glass. For most subjects the instrument was easily adjusted to achieve linearity for a 30° horizontal range and a 20° vertical range. This instrument uses an 85-Hz analog low-pass filter, producing records that are as linear, as low in noise, and as high in bandwidth as our standard photoelectric system [12].

The target was a small (3 mm in diameter) red laser dot projected on a white screen 172 cm in front of the subject. The target voltage drove a galvanometer that had a small mirror attached. The movement of the mirror deflected the laser beam to produce a moving dot on the screen. The bandwidths for the galvanometer and the DC amplifier exceeded 200 Hz. Subjects viewed the target binocularly in a dimly illuminated room (however vision was photopic).

Data were collected and analyzed with a PDP 11/34 minicomputer. Target and eye movement data were passed through a 12-bit analog-to-digital converter sampling at 1000 Hz, and the data were then filtered and stored on a disk for future calculations. Calibration factors were derived from segments of the data when the subject tracked a target that jumped between points $\pm 5^\circ$ from the primary position. Calibration factors for each eye were computed by averaging one to two seconds of data from four to ten manually selected periods when the eye was stationary and looking at the target.

Our digitized eye position records have a bandwidth of 80 Hz. The eye velocity was calculated with a two-point central difference algorithm [31]. The eye velocity records had 3-dB bandwidths of 8.9 Hz.

Vergence eye movements were eliminated by displaying the target on a screen a fixed distance from the head. It was speculated that the infrared mirror in front of the right eye might produce a Pulfrich illusion of motion in depth [32]. However, our subjects did not report seeing this effect. If they tried to track this illusion, vergence eye movements of less than two minutes of arc would have been necessary. Vestibulo-ocular movements were eliminated by restraining

the subjects' heads with a bite bar and a head rest. Smoothly moving targets were presented to elicit smooth-pursuit movements and minimize unwanted saccadic movements. Seven subjects participated in the experiments. Informed consent was obtained after the equipment and the experimental procedure had been explained.

Experimental Technique

In this study we opened the loop by adding an external electronic feedback loop that canceled the effects of the natural feedback loop (Fig. 2). While the subject tried to track a smoothly moving target, we measured eye position with the DDA oculometer and moved the target an angular distance equivalent to the eye movement. Thus eye movements became ineffective in correcting the retinal error, and the feedback loop was opened. However, after much trepidation, we conjecture that this technique only works for a few seconds, after which eye movements become capricious due to involvement of high-level cortical processes, such as the predictive mechanism mentioned earlier.

After calibration data had been taken, the subject was presented with five types of target waveforms: step displacements with the feedback loop opened; sine waves with the feedback loop closed; sine waves with the feedback loop opened; ramps with the feedback loop opened; and step-ramps with the feedback loop closed. The order of presentation was randomized to prevent prediction.

The step target was presented to the subject to verify that the technique of opening the loop using electronic feedback was working. Because the step target introduced a position error rather than a velocity error, this experiment involved the saccadic system rather than the pursuit system. A position error with the feedback loop opened should have elicited a staircase of saccades as shown in Fig. 3. If the expected open-loop response to the step target was seen, then the electronic feedback loop was opening the loop correctly.

The open and closed-loop sine waves were presented at 0.3, 0.5, 0.6, and 0.8 Hz. Different frequencies were used to determine if the data depended on target frequency. The amplitudes of the sine waves were usually $\pm 3^\circ$. Preliminary work indicated that with the feedback loop open, target amplitudes larger than 3° often elicited eye movements that went out of the $\pm 15^\circ$ linear range of the equipment. The eye movements of most subjects were within the $\pm 15^\circ$ range when smaller target amplitudes were used.

The triangular target waveform contained a series of rightward and leftward ramps with an amplitude of 5° and a frequency of 0.3 or 0.5 Hz. These ramp experiments were run with the feedback loop opened. Unfortunately, a saccade almost always camouflaged the start of smooth pursuit movements.

Therefore, we reverted to the step-ramp target waveform introduced by Rashbass [19]. Fig. 6 shows this step-ramp waveform. The target steps to one side and then ramps off

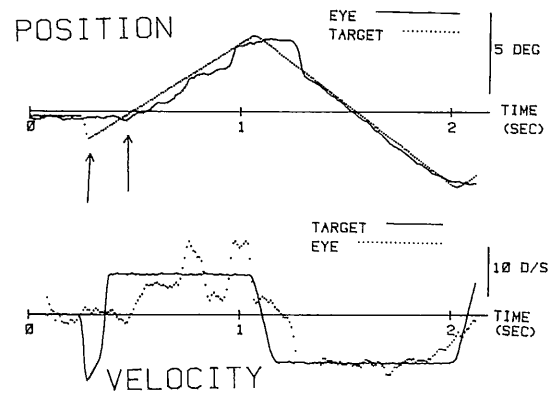


Fig. 6. Measurement of the smooth pursuit time delay from the closed-loop step-ramp waveform. The time delay corresponds to the time interval between the arrows.

in the opposite direction. Occurrence of saccades was minimized by making the time required for the target to return to its starting point equal to the latency of the saccadic system. A latency of 150 ms was assumed. With this waveform measurements were made in the first second of tracking, eliminating any responses due to the predictability of the target.

We had difficulty getting consistent results for open-loop sinusoids. As a result, most of our open-loop data came from either the first few seconds after the loop had been opened, or from the step-ramp waveform. Our difficulties with open-loop sinusoids were probably due to the involvement of the saccadic system and high cortical processes, such as prediction. Although we did not try them, we think that unpredictable waveforms, such as a sum of sinusoids or a pseudorandom sequence, should also eliminate these confounding cortical effects and yield consistent long-term open-loop tracking.

RECORDED DATA

From the experimental data, we measured the time delay of the saccadic branch, the time delay of the smooth pursuit branch, the ratio of the eye's velocity to the target's velocity, and the 10–90-percent rise time. We analyzed the data for each subject independently, but (except for the previously mentioned high open-loop gain of our most-experienced subject) we found no statistically significant intersubject differences. Therefore we only present the mean over all subjects and all experiments.

The time delay for the saccadic branch was measured from the open-loop step targets. With these targets, the eye made a series of saccades until saturation occurred. For these experiments, the intersaccadic delay was measured as well as the time between initial target movement and initial eye movement. Fig. 3 illustrates the data and measurements. The mean reaction time was 200 ms.

The data from the closed-loop sine waves and the closed-loop step-ramps gave values for the smooth-pursuit time delay. The delay corresponds to the time between the beginning of target movement and the beginning of pursuit

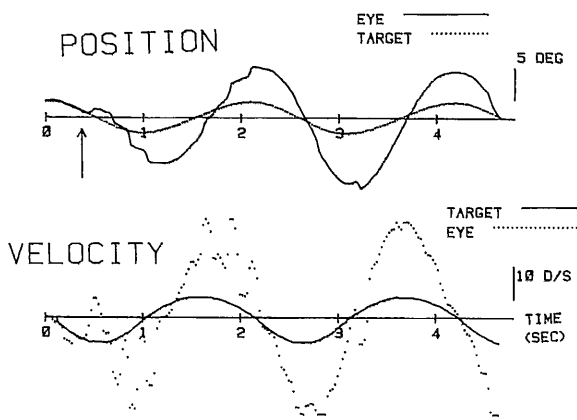


Fig. 7. Measurement of the velocity ratio from open-loop sine waves. The ratio of eye velocity to target velocity was computed at peak velocity. The arrow identifies the time when the feedback loop was opened.

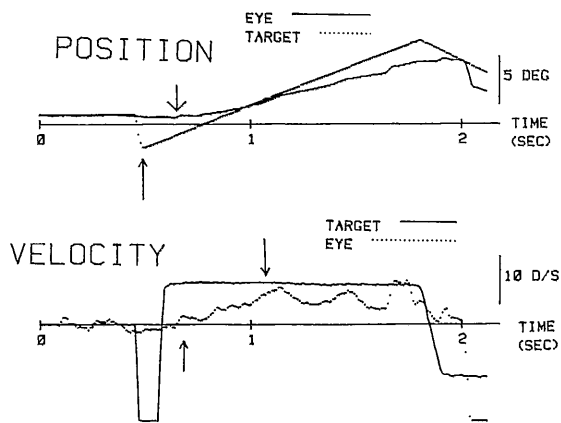


Fig. 8. Measurements from the closed-loop step-ramp data. The time interval between the arrows in the position trace is the time delay of the smooth pursuit system. The time between the arrows in the velocity trace is the 10-90-percent rise time.

movement as judged from the velocity trace. Fig. 6 shows the measurement of the smooth pursuit time delay from the step-ramp target waveform. The mean latency for the step-ramp target waveform was 171 ms. The mean latency for the sine waves was 176 ms.

The ratio of the eye's velocity to the target's velocity was measured from the open-loop sine wave data; this ratio is also called the open-loop gain. Fig. 7 shows a section of data used in computing this ratio. When the feedback loop was opened, the eye movements were larger than the target movements and (at this frequency) there was a phase lag of approximately 12°. This open-loop gain was found to have a mean value of 2.5.

The closed-loop step-ramps provided more data than the other waveforms. From this data we calculated the smooth pursuit branch's time delay, the 10-90-rise time, and the velocity ratio. Fig. 8 shows some step-ramp data. To calculate the rise time we first identified the point where the eye began tracking and the point where the eye reached a steady state velocity. The points corresponding to ten and 90 percent of the distance were marked and the time between them measured. The mean value of the 10-90-per-

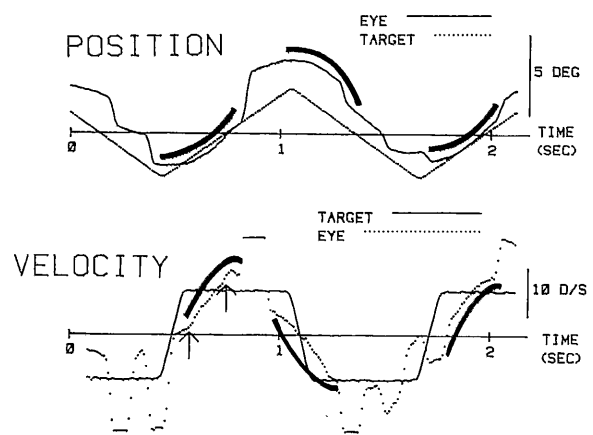


Fig. 9. Measurements from the open-loop ramp data. The time between the arrows is the 10-90-percent rise time. The thick parabola-like curves will be explained in conjunction with Fig. 10.

cent rise time was 96 ms. We also measured the ratio of the eye velocity to the target velocity after the transient. The mean velocity ratio was 0.67.

The open-loop ramp data also provided measurements of the rise time and open-loop gain. The rise time and velocity ratio measurements were made like those for the step-ramp experiments. The mean 10-90-percent rise time for the ramp experiments was 182 ms. For the velocity ratio a mean value of 1.61 was found. Fig. 9 shows some open-loop ramp data with the measurements.

The first five columns of Table I summarize the results of the raw data from each of the experiments. The time delays are reasonable; the large standard deviations are of biological, not experimental, origin. The two rise times differ because one comes from a closed-loop system and one from an open-loop system. The velocity ratios of open and closed loop systems also differ as expected. However, the large difference between the velocity ratio of the open-loop sine wave and the open-loop ramp was not expected (although they are within a standard deviation). We think the open-loop sine-wave data are bad, because their standard deviation was so large and because open-loop sine-wave experiments gave the least consistent results, both in the literature and in our experiments over a period of five years.

Comparison with the Literature

The time delay of the smooth pursuit branch has been measured by several groups. Rashbass [19] reported a delay of 150 ms; Robinson [14], 125 ms; and Young [26], 134 ms. These values all lie within one standard deviation of the 173-ms mean delay measured in this study. Our measurements for open-loop gain and most of the previously mentioned values in the literature range between two and four [5], [8], [9], [26].

The mean 10-90-percent rise time from the closed-loop step-ramp waveforms was 96 ms. Robinson [14] measured the total duration of movement for a step-ramp target to be 133 ms. A comparison can be made by computing the closed-loop time constant τ for each study. The time

TABLE I
MEAN AND STANDARD DEVIATION OF EXPERIMENTAL AND CALCULATED PARAMETERS¹

Experiment	Number of Experiments	Pursuit Time Delay	Velocity Ratio	Rise Time	Saccadic Time Delay	Gain	Time Constant
Sine wave Closed-loop	12	176 ms $\sigma = 57$ ms	-	-	-	-	-
Sine wave Open-loop	27	-	2.54 $\sigma = 1.11$	-	-	3.11 $\sigma = 1.24$	-
Step Open-loop	16	-	-	-	200 ms $\sigma = 30$ ms	-	-
Step-ramp Closed-loop	24	171 ms $\sigma = 57$ ms	0.67 $\sigma = 0.09$	96 ms $\sigma = 32$ ms	-	2.35 $\sigma = 1.05$	142 ms $\sigma = 51$ ms
Ramp Open-loop	6	-	1.61 $\sigma = 0.32$	182 ms $\sigma = 13$ ms	-	1.61 $\sigma = 0.35$	83 ms $\sigma = 6$ ms

¹For the smooth-pursuit system and the $K/(\tau s + 1)$ model.

measured by Robinson should equal three closed-loop time constants. This relationship gives a closed-loop time constant of 44.3 ms. The 10–90-percent rise time measured in our study equals 2.2 closed-loop time constants, therefore one closed-loop time constant equals 43.6 ms. So the closed-loop time constant measured in this study is the same as Robinson's.

For the closed-loop step-ramps our mean velocity ratio was only 0.67. Yet the literature abounds with examples of unity gain ramp tracking [19]–[23] as shown between the one and two second marks in Fig. 6. The major reason for this difference is prediction by the human. We used data from only the first second after the target started, thereby ignoring the unity gain tracking common for predictable targets. Thus our experimental data are in concert with data in the literature.

IDENTIFICATION OF THE MODEL

After the experimental data had been analyzed we turned our attention to developing a model that would fit the data. Various models were proposed for the smooth-pursuit branch, and the behavior of these models was compared to the experimental data. The model that most accurately simulated the experimental results was identified. The parameters of this model were then calculated, resulting in complete system identification.

Identification of Model's Form

The outputs of four linear models for the smooth pursuit system will be presented: a pure integrator (K/s), a first order lag (a leaky integrator) $K/(\tau s + 1)$, a critically damped second-order system, and an overdamped second-order system. We do not include more complicated systems, because these were sufficient to match human data and we wanted to keep the mathematics simple. For each model we compared its open-loop output to that of a human for several target waveforms. As previously noted, analyzing open-loop data is circular. A model is needed before one can completely analyze the data, but data are necessary to simulate the model. To derive the output of the models, we assumed a gain K of 2.5, a time constant τ

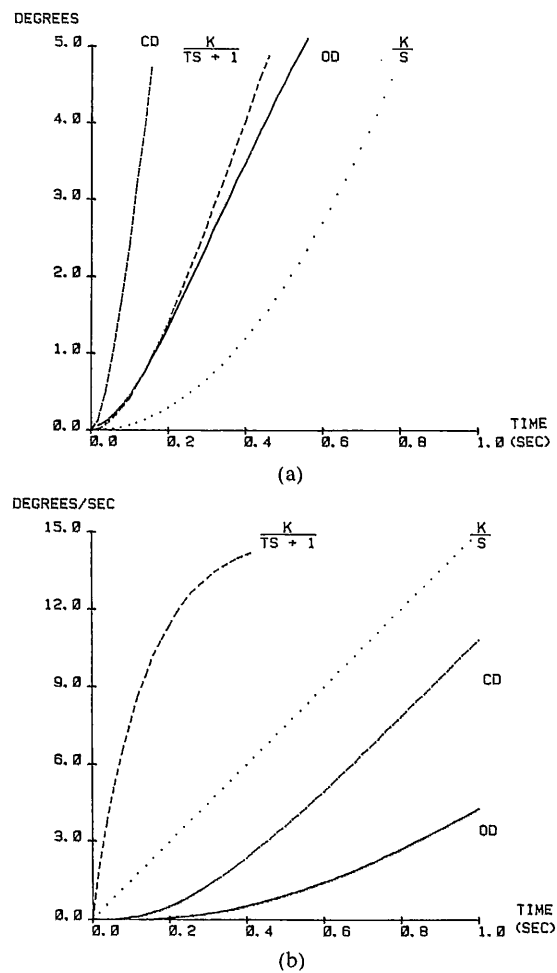


Fig. 10. (a) Position responses and (b) velocity responses for K/s , $K/(\tau s + 1)$, overdamped (OD), and critically damped (CD) models to an open-loop ramp target position input, which is a velocity step input. Human open-loop ramp data adjacent to the thick lines in Fig. 9 seem to match the $K/(\tau s + 1)$ model best.

of 140 ms, and for the overdamped case, a second time constant of 1 ms. Derivation of these values will be shown later; for the present they provide a means for comparing the output of the four models to human data.

Fig. 10(a) shows the position output of the four models for a ramp target. All four models have similar parabola-like

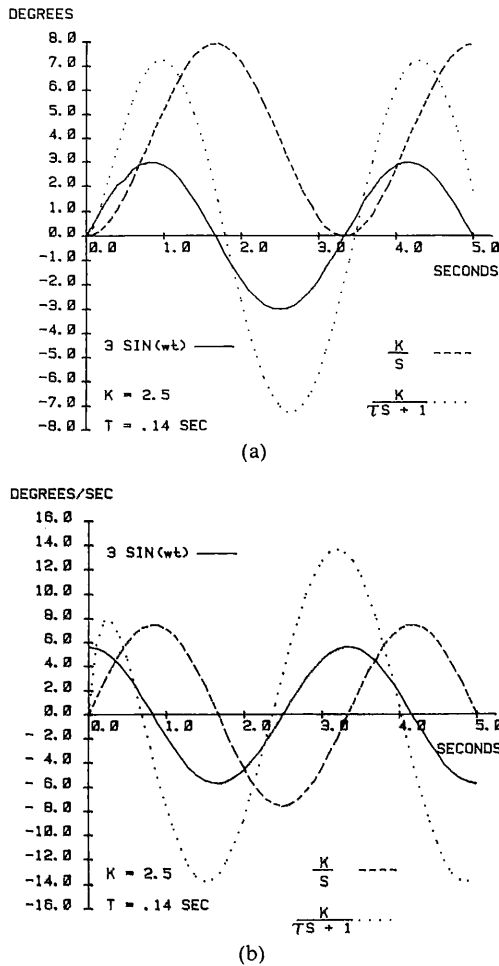


Fig. 11. (a) Position response and (b) velocity response for K/s and $K/(\tau s + 1)$ models to an open-loop sine wave. The human data of Fig. 7 best match the $K/(\tau s + 1)$ model.

shapes, so this type of an input is not useful for distinguishing between them. The human response has a similar shape as shown by the thick short parabolic segment drawn along side the eye movements in Fig. 9. In contrast, the bottom of Fig. 10 shows differences in the velocity outputs of the four models for a step change in the velocity input. The $K/(\tau s + 1)$ response starts with a positive slope and then approaches a steady-state saturation value. It is the only response with this shape. The human response seems to have a similar shape, as shown by the thick curves drawn along side the eye velocity curves in Fig. 9.

Similarly, the $K/(\tau s + 1)$ model provides the best match to the human open-loop sine-wave data. The position output of this model, shown in Fig. 11(a), has the large amplitude and a small phase lag seen in the human open-loop sine-wave experiments. In contrast the position output of the K/s model of Fig. 11(a) has an offset and a large phase lag, neither of which appear in the human data. The velocity curves in Fig. 11(b) also support the $K/(\tau s + 1)$ model. The $K/(\tau s + 1)$ model has a large amplitude and small phase lag as does the human velocity data of Fig. 7. Whereas the K/s model has a large 90° phase lag not seen in the data.

From these comparisons the model that most closely matches the experimental data is $K/(\tau s + 1)$. Adding the time delay gives the open-loop transfer function of

$$G_{ol} = \frac{Ke^{-sT}}{\tau s + 1}$$

Using this model, values for the parameters may now be computed.

Calculation of Model's Parameters Based on Experimental Data

The time delays were measured directly from the human data, but the system gain and time constant were calculated using human data and the proposed model.

First, the system gain and time constant were computed using values for the closed-loop gain and rise time from the step-ramp waveforms. For the human visual system the feedback element H is, of course, unity, because if the eye moves, the image on the retina moves by the same amount. So, ignoring the time delay, the model's closed-loop transfer function is

$$\frac{\dot{\theta}_E}{\dot{\theta}_T} = \frac{K}{\tau s + 1 + K} \tag{1}$$

where $\dot{\theta}_E$ represents eye velocity; $\dot{\theta}_T$, target velocity; K , the system gain; τ , the time constant; and s , the angular frequency of the target. A step input for the target velocity (a ramp input for the target position) gives $\dot{\theta}_T = 1/s$. Substituting $\dot{\theta}_T = 1/s$ into (1) gives an output in the frequency domain of

$$\dot{\theta}_E = \frac{K}{s(\tau s + 1 + K)} \tag{2}$$

This yields an output in the time domain of

$$\dot{\theta}_E(t) = \frac{K}{1 + K}(1 - e^{-(1+K)t/\tau}) \tag{3}$$

where the term $K/(1 + K)$ is the velocity ratio. Using the 0.67 value measured from the human step-ramp data yields a gain K of 2.3.

The computation for the time constant was done in the following way. The closed-loop time constant of (3) is $\tau_{CL} = \tau/(1 + K)$. The rise time for our first order model obeys the relationship $T_R = 2.2 \tau_{CL}$. Therefore, it follows that

$$\tau = \frac{(1 + K)T_R}{2.2} \tag{4}$$

The time constant was computed using (4), the just derived system gain of 2.3, and the measured rise time T_R . The mean time constant was 142 ms.

Next the open-loop ramp data were analyzed. Ignoring the time delay once again, the open-loop transfer function for the proposed model is

$$\frac{\dot{\theta}_E}{\dot{\theta}_T} = \frac{K}{\tau s + 1} \tag{5}$$

A ramp input, corresponding to a step velocity input, gives

$$\dot{\theta}_E = \frac{K}{s(\tau s + 1)}. \quad (6)$$

Taking the inverse Laplace transform, $\dot{\theta}_E(t) = K(1 - e^{-t/\tau})$. Therefore, the velocity ratio measured directly from the open-loop ramp data is the gain of the pursuit branch. The mean was 1.61. The time constant for this experiment was computed, once again, using $\tau = T_R/2.2$. This equation gave a mean time constant of 83 ms.

Computing the gain from the open-loop sine-wave data required using the time constant derived from another experiment. Because this was open-loop data, we used the 83-ms time constant from open-loop step-ramps. The open-loop transfer function was once again given by (5), which can be rearranged as

$$K = (\tau s + 1) \frac{\dot{\theta}_E}{\dot{\theta}_T} \quad (7)$$

from which the mean gain of 3.1 was computed. However, as previously stated, we do not have confidence in the open-loop sine-wave data. Having to use a time constant derived from a different experiment further lessens our confidence in this value.

The last two columns of Table I list the mean and standard deviation of the computed parameters for each experiment. The only other model to use the $K/(\tau s + 1)$ plant was that reported by Young [26]. They used a time constant of 40 ms and a gain of one. To compare our results with their results, we recomputed our time constant assuming a gain of one. The mean 10–90-percent rise time from the step-ramp experiments was 96 ms. Using (4), τ was found to be 87 ms. The open-loop ramp experiments gave a time constant independent of the system's gain. The value for the time constant from these experiments was 83 ms. Thus both of our results are about twice the value used by Young *et al.*

Final Smooth-Pursuit Model

To use the average parameter values in the model would be failing to acknowledge the biological noise in the data and would imply a false confidence in those values. Therefore, the average values were rounded off to provide the following "nice" numbers for the model: $K = 2.0$, $T = 150$ ms, and $\tau = 130$ ms. Thus the complete smooth-pursuit model became

$$G_{ol} = \frac{2e^{-.15s}}{0.13s + 1}. \quad (8)$$

The resulting model tracks like a human as shown in Fig. 12. However, this model is only marginally stable. If K was increased (or if the numerical algorithms for integration, differentiation, and summation produced phase shifts) then the model became unstable. This means that experimental data showing open-loop gains greater than two imply a change in time delay or control strategy.

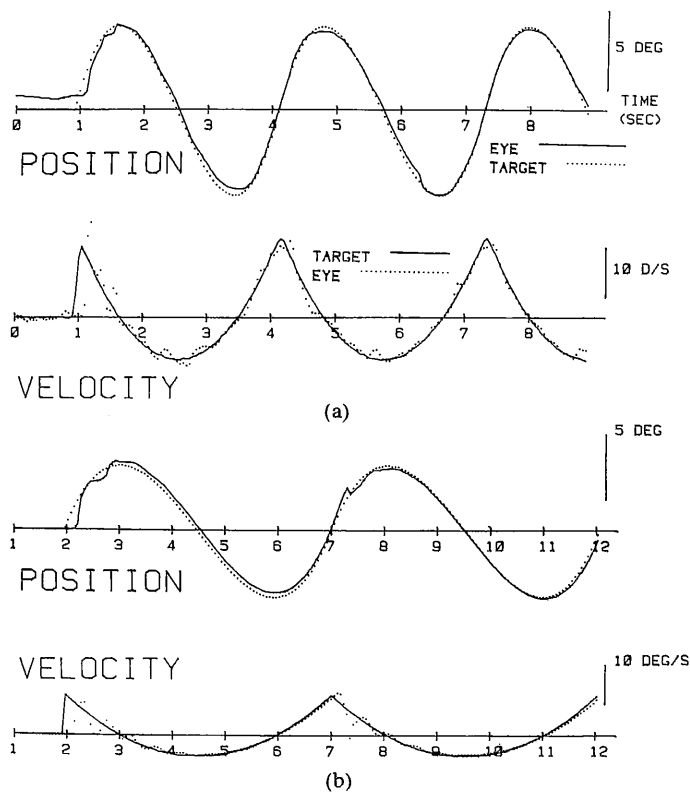


Fig. 12. Comparison of (a) human and (b) model (bottom) tracking of a cubical waveform. Both start out with a couple of position correcting saccades and at a quarter of a cycle they settle down to zero-phase tracking. Small position errors that develop are eliminated by small saccades. The unusual cubical waveform is being accurately tracked (and not just approximated with a sinusoid) as can be seen from the velocity traces.

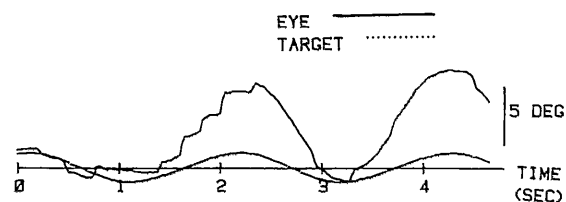


Fig. 13. Position response for human open-loop tracking. After the feedback loop was opened, at the 1-s mark, the subject made a series of saccades trying to catch the target. When this strategy did not work, he seemed to turn off the saccadic system, and produced only smooth pursuit movements. This subject was experienced in oculomotor experiments, which explains the large open-loop gain.

A sensitivity analysis of the closed loop model showed that the mean squared error between the model and the target decreased as the time delay decreased, as the time constant decreased, and as the gain increased (until the system became unstable). These three parameters had equivalent effects on the transient response and no effect on the steady-state tracking; that is, all three sensitivity functions went to zero after three seconds.

DISCUSSION

We cautioned earlier that open-loop experiments were difficult to perform, because when the experimenters threw the switch that supposedly opens the loop, they also altered

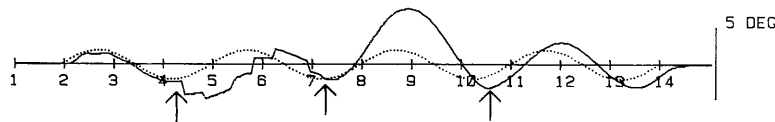


Fig. 14. Model (solid) tracking a sinusoidal target (dotted) under a variety of conditions. At the first arrow the loop was opened, at the second arrow the saccadic system was turned off, at the third arrow the adaptive controller was turned off. Tracking patterns similar to each of these are common in human records.

the behavior of the target. Often the subjects would detect this change in target behavior and change their tracking strategies. Fig. 13 shows an example of such a change in human tracking strategy. For the first half of this record the subject behaved as one would expect for a subject tracking an open-loop target; there is a saccade every 200 ms. However, in the middle of the record the saccades cease; it seems that the subject turned off the saccadic system. Such saccade free tracking was common in our experiments and in other open-loop experiments [5]–[9]. It is odd that previous open-loop experimenters did not comment on this strange lack of saccades in their data. The records are strikingly devoid of saccades in spite of the large position errors.

In Fig. 14 we show our model tracking the target. From 2 to 4.25 s there is a normal closed-loop tracking. At 4.25 s we opened the loop, turned off the adaptive controller, and reduced the smooth pursuit gain to 0.7, thus producing a staircase of saccades similar to those shown in Fig. 13. At 7.25 s we turned off the saccadic system, turned the adaptive controller back on, and returned the gain of the smooth pursuit system to its normal value; the model tracked with an offset similar to that of Fig. 13. We often noticed this type of position offset in our human subjects during open-loop tracking. Finally, at 10.5 s we turned off the adaptive controller, and the model tracked without an offset like the human tracking of Fig. 7.

These simulations help explain some confusing data in the literature by allowing us to suggest that when the loop on the human smooth-pursuit system is electronically opened, some subjects continue to track with all systems (producing a staircase of saccades), some turn off the saccadic system (producing smooth tracking with an offset), some also turn off the adaptive controller (producing smooth tracking without an offset), and some change the gain on the smooth-pursuit system. This is an important aspect of our study; running experiments on the model that were not used to design the model. The results of these simulations taught us that the human brain has great variability.

SUMMARY

In order to open the loop on a system using electronic feedback, all other systems must be eliminated. We eliminated the vestibulo-ocular and vergence systems by fixing the subject's head and by keeping the target at a constant distance. The step-ramp waveform eliminated the need for the saccadic system. The most difficult systems to be removed were the high level cortical processes, such as

the prediction elements. We obtained our best results studying eye movements just after unpredictable target motions, such as in the first few seconds after opening the loop.

The open-loop transfer function of the human smooth system can be modeled as

$$G_{ol} = \frac{2e^{-.15s}}{0.13s + 1}$$

The form of this model was chosen after comparing human data to proposed models for the system and selecting the model that most closely approximated the human data. Based on this form the numerical parameters were then calculated from the experimental data: one of the most important features of the model is that it is a simple linear system. This model was then compared to model and human results by other experimenters and found to be consistent with their results.

When the above model was incorporated into the more encompassing TSAC model, the computer simulations emulated both open- and closed-loop human tracking, including overcoming a time delay and producing zero-latency tracking of predictable targets. Although the model certainly is not unique, it is the only published model that can emulate the human in all of these experimental conditions.

But the purpose of modeling is not to build a model; modeling should teach something about the physical system. Results of running this model led us to suggest that when tracking predictable targets in the open-loop condition, humans sometimes turn off their adaptive controller, humans sometimes turn off their saccadic system, and humans sometimes change the gain on their smooth pursuit system. In other words, they change their control strategy.

ACKNOWLEDGMENT

We thank the reviewers for their sage comments and Steve Oakley for making Fig. 4.

REFERENCES

- [1] A. T. Bahill and J. D. McDonald, "Smooth pursuit eye movements in response to predictable target motions," *Vision Res.*, vol. 23, pp. 1573–1583, 1983.
- [2] A. T. Bahill and T. LaRitz, "Why can't batters keep their eyes on the ball?" *American Scientist*, vol. 72, pp. 249–253, 1984.
- [3] H. J. Wyatt and J. Pola, "Slow eye movements to eccentric targets," *Invest. Ophthalmol. Vis. Sci.*, vol. 21, pp. 477–483, 1981.
- [4] S. G. Lisberger, C. Evinger, G. W. Johanson, and A. F. Fuchs, "Relationship between eye acceleration and retinal image velocity

- during foveal smooth pursuit in man and monkey," *J. Neurophysiol.*, vol. 46, pp. 229-249, 1981.
- [5] M. F. W. Dubois and H. Collewijn, "Optokinetic reactions in man elicited by localized retinal motion stimuli," *Vision Res.*, vol. 19, pp. 1105-1115, 1979.
- [6] H. J. Wyatt and J. Pola, "The role of perceived motion in smooth pursuit eye movements," *Vision Res.*, vol. 19, pp. 613-618, 1979.
- [7] A. Mack, R. Fendrich, and E. Wong, "Is perceived motion a stimulus for smooth pursuit?" *Vision Res.*, vol. 22, pp. 77-88, 1982.
- [8] R. J. Leigh, S. A. Newman, D. S. Zee, and N. R. Miller, "Visual following during stimulation of an immobile eye (the open loop condition)," *Vision Res.*, vol. 22, pp. 1193-1197, 1982.
- [9] H. J. Wyatt and J. Pola, "Smooth pursuit eye movements under open-loop and closed-loop conditions," *Vision Res.*, vol. 23, pp. 1121-1131, 1983.
- [10] W. B. Cushman, J. F. Tangney, R. M. Steinman, and J. L. Ferguson, "Characteristics of smooth pursuit eye movements with stabilized targets," *Vision Res.*, vol. 24, pp. 1003-1009, 1984.
- [11] L. Stark, *Neurological Control Systems, Studies in Bioengineering*. New York: Plenum, 1968.
- [12] A. T. Bahill, *Bioengineering: Biomedical, Medical and Clinical Engineering*. Englewood Cliffs, New Jersey: Prentice-Hall, 1981.
- [13] L. R. Young and L. Stark, "Variable feedback experiments testing a sampled data model for eye tracking movements," *IEEE Trans. Human Factors Electron.*, vol. HFE-4, pp. 38-51, 1963.
- [14] D. A. Robinson, "The mechanics of human smooth pursuit eye movements," *J. Physiol.*, vol. 180, pp. 569-591, 1965.
- [15] J. S. Brodkey and L. Stark, "New direct evidence against intermittency or sampling in human smooth pursuit eye movements," *Nature*, vol. 218, pp. 273-275, 1968.
- [16] J. D. McDonald, A. T. Bahill, and M. B. Friedman, "An adaptive control model for human head and eye movements while walking," *IEEE Trans. Syst., Man., Cybern.*, vol. SMC-13, pp. 167-174, 1983.
- [17] J. D. McDonald and A. T. Bahill, "Zero-latency tracking of predictable targets by time-delay systems," *Int. J. Control*, vol. 38, pp. 881-893, 1983.
- [18] —, "Model emulates human smooth pursuit system producing zero-latency target tracking," *Biol. Cybern.*, vol. 48, pp. 213-222, 1983.
- [19] C. Rashbass, "The relationship between saccadic and smooth tracking eye movements," *J. Physiol.*, vol. 159, pp. 326-338, 1961.
- [20] L. Schalen, "Quantification of tracking eye movements in normal subjects," *Acta Otolaryngol.*, vol. 90, pp. 404-413, 1980.
- [21] R. D. Yee, S. A. Daniels, W. J. Oliver, R. W. Baloh, and V. Honrubia, "Effects of an optokinetic background on pursuit eye movements," *Invest. Ophthalmol. Vis. Sci.*, vol. 24, pp. 1115-1122, 1983.
- [22] J. van der Steen, E. P. Tamminga, and H. Collewijn, "A comparison of oculomotor pursuit of a target in circular real, beta or sigma motion," *Vision Res.*, vol. 23, pp. 1655-1661, 1983.
- [23] E. Kowler, J. van der Steen, E. Tamminga, and H. Collewijn, "Voluntary selection of the target for smooth pursuit eye movement in the presence of superimposed full-field stationary and moving stimuli," *Vision Res.*, vol. 24, pp. 1789-1798, 1984.
- [24] R. Eckmiller, "Neural control of foveal pursuit versus saccadic eye movements in primates—single unit data and models," *IEEE Trans. Syst., Man, Cybern.*, vol. SMC-13, pp. 980-989, 1983.
- [25] D. H. Fender and P. W. Nye, "An investigation of the mechanisms of eye movement control," *Kybernetik*, vol. 1, pp. 81-88, 1961.
- [26] L. Young, "Pursuit eye tracking movements," in *The Control of Eye Movements*, P. Bach-y-Rita, C. C. Collins, and J. Hyde, Eds. New York: Academic, 1971, pp. 429-443.
- [27] S. Yasui and L. Young, "Perceived visual motion as effective stimulus to pursuit eye movement system," *Science*, vol. 190, pp. 906-908, 1975.
- [28] L. R. Young, "The sampled data model and foveal dead zone for saccades," in *Models of Oculomotor Behavior and Control*, B. L. Zuber, Ed. Boca Raton, Florida: CRC, 1981, pp. 43-74.
- [29] M. Steinbach, "Pursuing the perceived rather than the retinal stimulus," *Vision Res.*, vol. 16, pp. 1371-1376, 1976.
- [30] M. Bach, D. Bouis, and B. Fischer, "An accurate and linear infrared oculometer," *J. Neurosci Methods*, vol. 9, pp. 9-14, 1983.
- [31] A. T. Bahill and J. D. McDonald, "Frequency limitations and optimal step-size for the two-point central difference derivative algorithm with applications to human eye movement data," *IEEE Trans. Biomed. Engr.*, vol. BME-30, pp. 191-194, 1983.
- [32] H. Ono and M. Steinbach, "The Pulfrich phenomenon with eye movement," *Vision Res.*, vol. 23, pp. 1735-1737, 1983.